Computers and Concrete, *Vol. 26, No. 2 (2020) 151-159*
DOI: https://doi.org/10.12989/cac.2020.26.2.151

Computer modeling and analytical prediction of shear transfer in reinforced concrete structures

Marcela N. Kataoka*[1], Ana Lúcia H.C. El Debs[1a], Daniel de L. Araújo[2b] and Bárbara G. Martins[2c]

[1]Structural Department, Engineering School of São Carlos, University of São Paulo, Av. Trabalhador, Saocarlense, nº 400, CEP: 13566-580 São Carlos, SP, Brazil
[2]School of Civil and Environmental Engineering, Federal University of Goiás, Universitária Street, nº 1488, Qd 86, Setor Universitário, Goiânia, GO 74605-220, Brazil

(*Received July 2, 2019, Revised July 27, 2020, Accepted July 28, 2020*)

Abstract. This paper presents an evaluation of shear transfer across cracks in reinforced concrete through finite element modelling (FEM) and analytical predictions. The aggregate interlock is one of the mechanisms responsible for the shear transfer between two slip surfaces of a crack; the others are the dowel action, when the reinforcement contributes resisting a parcel of shear displacement (reinforcement), and the uncracked concrete comprised by the shear resistance until the development of the first crack. The aim of this study deals with the development of a 3D numerical model, which describes the behavior of Z-type push-off specimen, in order to determine the properties of interface subjected to direct shear in terms cohesion and friction angle. The numerical model was validated based on experimental data and a parametric study was performed with the variation of the concrete strength. The numerical results were compared with analytical predictions and a new equation was proposed to predict the maximum shear stress in cracked concrete.

Keywords: shear strength; finite element modeling; aggregate interlock; push-off test; Z-type specimen, numerical analysis

1. Introduction

The aggregate interlock is a complex mechanics of shear transfer, which involves the interaction between normal and shear stresses. Normal stresses are introduced at the crack faces if its opening is restricted by reinforcement. In addition, the shear strength decreases with the opening of the cracks due to the loss of contact between the faces. According to Spinella (2013), Lee *et al*. (2014), Arani *et al*. (2019) the use of fibre reinforcement enhances shear resistance by bridging tensile normal stresses across diagonal cracks and reducing diagonal crack spacing and width, which increases aggregate interlock effect.

In order to acquire more information about shear transfer in reinforced concrete elements, different types of direct shear tests have been adopted to investigate the shear capacity. The following types of specimens are used to investigate direct shear behavior:

a) Z-type
b) Double notched specimen
c) FIP-type

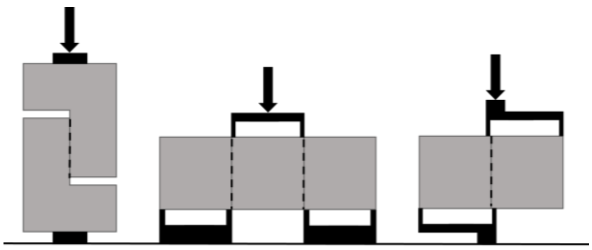

Fig. 1 Different test setups used to investigate the direct shear transfer: (a) Z-type, (b) JSCE-type and (c) FIP-type

All of the three prototypes were designed in order to reduce the effect of bending and to achieve a pure state of shear. *Z*-type specimens were used by Hamadi and Regan (1980), Walraven and Reinhardt (1981), Sagaseta and Vollum (2011), Xiao *et al*. (2014), Xu *et al*. (2015), Xiao *et al*. (2016), Rahal *et al*. (2016), Sun *et al*. (2018), Wu *et al*. (2019) to investigate the fundamentals of aggregate interlock and the shear-friction response of concrete with reinforcement crossing the shear plane. In precast concrete structures, the *Z*-type specimens were already used to study the behavior of shear keys, as the research of Bu *et al*. (2018), Jang *et al*. (2018). The shear key represents the interlocking resistance, an important mechanism of shear transfer in dry joints between column and beam.

Due to the additional reinforcement required in the two *L*-shaped concrete blocks (Fig. 1(a)), it is difficult to cast these specimens. To simplify the experimental program, a

*Corresponding author, Professor
E-mail: kataoka@sc.usp.br
[a]Professor
E-mail: analucia@sc.usp.br
[b]Professor
E-mail: dlaraujo@ufg.br
[c]Ms.c.
E-mail: barbaragm.civil@gmail.com

http://www.techno-press.org/?journal=cac&subpage=8
ISSN: 1598-8198 (Print), 1598-818X (Online)

double notched standard specimen (Fig. 1(b)) has been used by researchers. This test setup is based on the Japanese standard JSCE (2005). The third specimen type is a single notched prism, which is prescribed by FIP (1978) (Fig. 1(c)).

According to Soetens and Matthys (2017) when the shear capacity is determined by means of the modified JSCE test, higher shear stresses are observed compared to the tests with *Z*-type specimens.

Modelling aggregate interlock is a strenuous work owing the difficulties in defining roughness of the faces of the crack, in the evaluation of the effect of localized stresses around embedded steel bars, normal stresses and dowel action. According to Swamy and Andriopoulos (1974), Taylor (1970), studies showed that the aggregate interlock mechanism contributes between 30% and 90% to the postcracking shear resistance of the concrete.

The shear strength of concrete is the result of a combination of various mechanisms. ASCE-ACI Committee 445 (1998) mentions three shear mechanisms, which are related to the ultimate concrete shear resistance. The shear resistance is maintained by:

• uncracked concrete in cracked elements or until the development of first shear crack;

• aggregate interlock mechanism between two slip surfaces of a crack. The shear resistance by aggregate interlock depends on the crack opening and the roughness of the slip surfaces;

• dowel action occurs when the longitudinal steel reinforcement bars resist part of the shear displacement by dowel forces.

In the design of reinforced concrete structures, there are many different situations where transfer of shear across a specific plane needs to be considered. Such problem may be divided into two distinct categories: transfer of shear across an uncracked plane and across a cracked plane.

In a number of research has been studied the shear friction parameters of initially cracked concrete sliding planes have been worked on. The presence of a crack along the shear plane prior to the application of the load prevents the development of a truss action.

Under shear, one side of the crack slips relative to the other. Due to the roughness and irregularities that exist along the crack, this slip appears together with the crack opening. As a result, the reinforcing bars crossing the cracked shear plane are activated and experience normal stresses.

However, the shear is maintained by friction in the sliding faces, by the resistance offered by the protuberances on the crack faces and by dowel action of the steel bars crossing the crack. This is the basis of the shear-friction theory for the evaluation of the capacity of a crack transmitting shear forces in structural concrete.

International standards, such as EN 1992-1-1- Eurocode 2 (2004) and ACI Committee 318 (2008) prescribe that the Coulomb failure criteria (Eq. (1)) can determine the maximum shear stress (τ) transferred through aggregate interlock. The cohesion factor (c) is defined in terms of the concrete tensile strength and the coefficient of friction (μ) is correlated to the roughness of the interface.

$$\tau = c + \mu\sigma \tag{1}$$

Based on extensive research on shear friction, it is stated in reference Santos and Júlio (2012) that the roughness of the concrete substrate has a very significant influence on the bond strength of concrete-to-concrete interfaces. This aspect is considered in the design expressions in the form of the coefficients of cohesion and friction.

There are large variations in the values of cohesion factor (c) and coefficient of friction (μ) recommended in the literature. Based on statistical evaluation, it is proposed in reference Mattock (1974) that c=2.8 MPa and tan μ= 0.8. In reference Climaco and Regan (2001) an expression was developed to determine the cohesion factor (c), which is dependent of the compressive strength and the roughness of the crack faces. Eq. (2) is given for rough interfaces and the suggested coefficient of friction (μ) is 1.4.

$$c = 0.25(f_c)^{2/3} \tag{2}$$

Based on experimental results and analytical studies, empirical equations to calculate the maximum shear stress were suggested by several researches. In Patnaik (2000) the following expression of Eq. (3) is proposed for the prediction of the ultimate shear stress of not intentionally roughened surfaces for monolithic concrete.

$$\tau = 0.5\sqrt{(0.25 + \rho f_y) f_c} \tag{3}$$

In Kahn and Mitchell (2002), a study was carried out to evaluate the shear-friction prescriptions of the ACI 318 (1999) for high strength concretes. The proposed equation (Eq. (4)) can be used for normal and high strength concretes with monolithic concrete connections.

$$\tau = 0.05 f_c + 1.4\rho f_y \tag{4}$$

Z-type push-off specimens were employed in Mansur *et al*. (2008) to investigate the shear transfer across a crack, both analytically and experimentally. A comparison between several design expressions was made and according to the results, the Eq. (5) was proposed to determine the maximum shear (τ).

$$\tau = 0.56 f_c^{0.615} + 0.55\rho f_y \tag{5}$$

The variables of Eqs. (3), (4) and (5) stand for the same properties: ρ is the reinforcement ratio; f_y is the yield strength of the reinforcement; and f_c is the concrete compressive strength.

This study is intended to contribute to the studies on shear transfer through cracks with the development of a numerical model capable of representing the behavior of a *Z*-type push-off specimens. The numerical model was validated with experimental data and a parametric study was carried out. The results were compared with theoretical predictions, which provided satisfactory agreement.

2. Experimental analysis

In this research, the experimental results of shear transfer across cracks in reinforced concrete were obtained in tests with *Z*-type push-off specimen. The experimental program was developed by Martins (2016). Three push-off

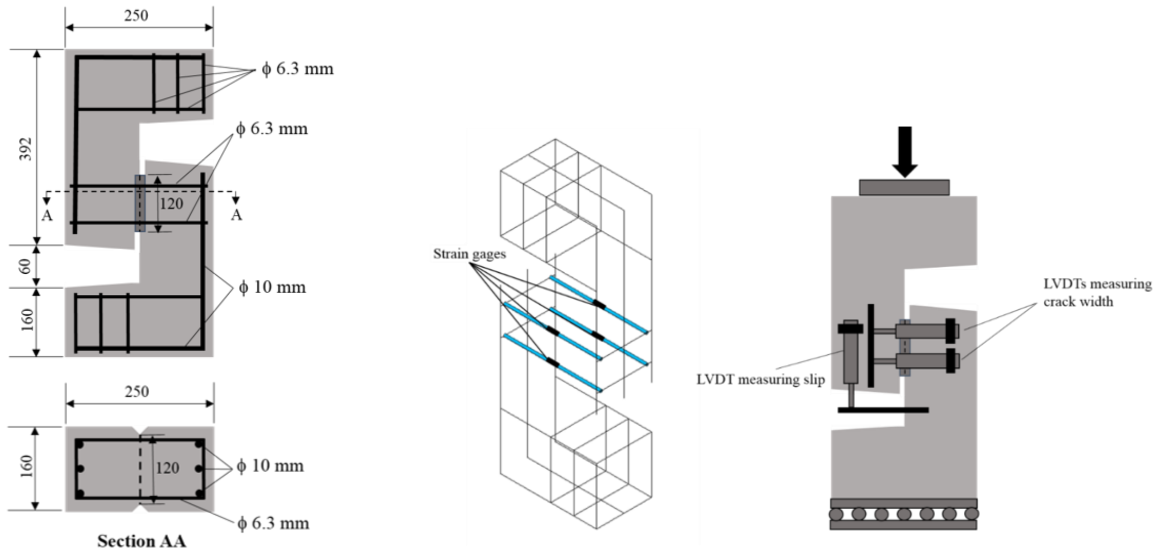

(a) Dimensions and reinforcement (b) Instrumentation

Fig. 2 Details of the prototype used by Martins (2016) (Unit: mm)

Table 1 Composition of the concrete matrix

Material	Quantity (kg/m³)
Equivalent cement	508
Cement - CP II F 40	483
Water	182
active silica	19
Natural sand	379
Artificial sand	350
Aggregate 12.5 mm	836
Superplasticizer	8.69
Water/cement ratio w/c	0.38

Table 2 Concrete properties in push-off tests

Properties	Value
Specific weight (kg/m³)	2262.5
Cone trunk rebate (mm)	80
f_{cm} (MPa)	66.29
f_{ctm} (MPa)	5.18
E_{cm} (GPa)	37.96

tests were conducted to investigate the influence of aggregate interlock on shear transfer through cracks. The *Z*-type specimens had cross-section of 160 mm×250 mm and total length of 612 mm. The geometry, dimensions and reinforcement details of the specimens are shown in Fig. 2(a).

Both blocks of the specimen were reinforced with three ϕ10 mm longitudinal bars and three ϕ6.3 mm transverse stirrups tied together for avoiding the specimen failure at the point of loading. Two stirrups with a diameter of ϕ6.3 mm were placed through the shear plane. This reinforcement has the function of guaranteeing the transmission of the normal stress to the plane of shear when the two faces of the crack slides. To minimize the contribution of the dowel action of this reinforcement on the shear plane strength, the adhesion between the reinforcement and the concrete was removed. Before performing the push-off tests, a splitting crack was introduced in each specimen along the shear plane by placing it in a horizontal position and applying a line load through a pair of steel wedges.

In the push-off tests, the slip of one block of the specimens relative to the other was measured by two LVDTs (Fig. 2). Two more LVDTs were mounted horizontally to measure lateral displacement, one on each side of the specimen. The strains in the stirrups in the region of the shear plane were measured by means of strain gages (Fig. 2(b)). The loading speeds adopted were 0.004 mm/min up to three minutes; 0.02 mm/min until reaching the maximum load and 0.05 mm/min until the end of the test.

The results of the material tests for the concrete used in the specimens are presented in Table 1 (the composition of the concrete matrix) and Table 2, which present the average values of the mechanical concrete properties.

3. Numerical analysis

3.1 Numerical model

The numerical analysis proposed in this paper is focuses on verifying that the numerical modelling is a potential tool to satisfactorily replicate the experimental push-off test with *Z*-type specimen.

The numerical simulation is an inexpensive alternative to structural analysis due to the fact that replaces the physical tests, which are expensive and time-consuming to be built. To validate the simulation results the numerical data were compared with experimental results. 3D finite element models were created for replicating the push-off tests of the experimental program of Martins (2016). The software Midas FX+ was used to construct the geometry and also to view the results (pre and post processing). The TNO DIANA software was used to process the numerical model using the finite element method (FEM).

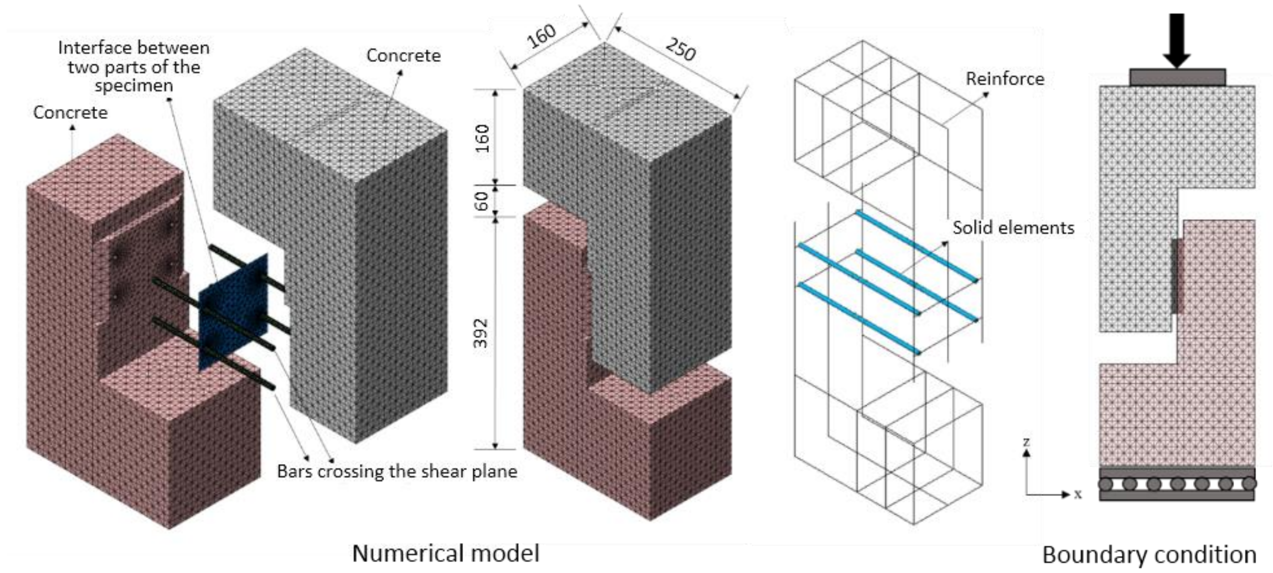

Fig. 3 Details of push-off *Z*-type numerical model (Unit: mm)

The main purpose of the paper is to evaluate the shear transfer across the cracks in reinforced concrete and it is done considering between the two *L*-shaped concrete blocks of the model. An interface was also introduced between concrete and the bars crossing the shear plane, due to elimination of adhesion in the physical model. The concrete and the stirrups crossing the shear plane were described with solid finite elements and the rest of the steel bars was defined as REINFORCE, which is a DIANA tool that simulates a presence of rebars. Details of the numerical model are shown in Fig. 3.

Different densities of mesh were tested in order to match the quality of the results with the time spent in processing. However, the mesh with elements with 10 mm in dimension was selected due to the good compromise between the size of the elements and the stability of the numerical solution.

The boundary conditions adopted for the numerical model were restriction of the displacements in y and z directions of the bearing plane, simulating the same conditions of the test. Loading was introduced at the top of the specimen. The boundary condition is presented in Fig. 3.

3.2 Finite elements

Two types of finite elements were used to construct the mesh: elements of plane stress and interface elements. The plane state elements were used to describe the concrete and the stirrups crossing the shear plane, while the interface elements were used at the shear interface and between stirrups and concrete.

Solid elements TE12L were used for the concrete. They are four-nodded, three-faced isoparametric solid pyramids with three degrees of freedom. The interface element used is T18IF, which has 3 + 3 nodes and comprising two planes in a three-dimensional configuration with three degrees of freedom. The illustrations of the two types of finite elements is shown in Fig. 4 and they are as described in the manual (TNO DIANA, 2009).

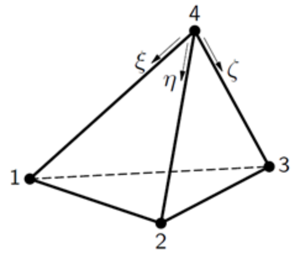

TE12L

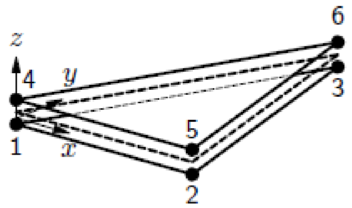

T18IF

Fig. 4 Finite elements used in the numerical model (TNO DIANA 2009)

3.3 Materials

3.3.1 Properties

The mechanical properties of the concrete, compressive strength, tensile strength and Young's modulus applied in the numerical analyses are the values determined in the experimental program. For the reinforcing bars, the nominal properties were used: Young's modulus is 210 GPa and yield strength 500 MPa.

3.3.2 Constitutive models

• *Concrete*

The selection of the most appropriate failure criterion according to the structural materials is a prerequisite in nonlinear analysis. The constitutive model adopted to describe the concrete elements was the Mohr Coulomb. Owing their simplicity and obtaining of more accurate results, Mohr Coulomb criterions became the most commonly used failure criterions for concrete and reinforced concrete. Mohr Coulomb criterion is presented as Eq. (6).

$$\tau = c + tan\,\phi\,\sigma \tag{6}$$

In Eq. (6), τ, c, σ, and ϕ are defined as shear strength, cohesion, normal stress, and internal friction angle, respectively. The accuracy of the nonlinear analysis depends on the accuracy of these parameters. From the existing technical literature it can be seen that many different values have been proposed for cohesion and internal friction angle by different researchers. According to Chen (1982), the friction angle ranges from 30 to 56.6° for different concrete elements. In Nielsen (1999) it is concluded that the friction angle varies from 37° for low-strength concrete to a constant value of 28° for concrete strengths greater than 65 MPa.

In reference Cela (1998), the relationship between the material parameters (cohesion c and friction angle ϕ) and the compressive and tensile strength of the concrete has been developed in the form given as Eqs. (7) and (8) below.

$$c = f_c\left(\frac{1-\sin\phi}{2\cos\phi}\right) \tag{7}$$

$$\phi = sin^{-1}\left(\frac{f_c - f_t}{f_c + f_t}\right) \tag{8}$$

Table 3 presents the values of cohesion (c) and friction angle (ϕ) used in the numerical model for concrete plain.

• *Doweling rebars*

The steel bars were described by the plasticity models of Von Mises, which are appropriate for ductile materials. The Von Mises model of maximum energy distortion was chosen for the steel elements in this model under the assumption that the maximum energy accumulated in the distortion of the material cannot exceed the maximum distortion energy for the same material in an axial tensile test.

• *Reinforcement*

The reinforcement excluding the doweling bars crossing the shear plane, was represented by REINFORCE, which is a tool of the software DIANA specific to simulate the behavior of steel bars. The finite element crossed by the REINFORCE is stiffened, which causes the same effect that stirrups cause in reinforced concrete structures. The plasticity models of Tresca and von Mises are applicable to steel elements because they are ductile materials. The model of maximum energy distortion of Von Mises was chosen for the reinforcement. This model admits that the maximum energy accumulated in the distortion of the material cannot exceed the maximum distortion energy for the same material in an axial tensile test.

• *Interface*

In the numerical model, two types of interface were employed - the first one between the doweling bars and concrete is based on bond slip and the second one between the two L-shaped concrete blocks comprising the shear plane is based on Coulomb friction. The Bond Slip interface was adopted due to the absence of adhesion between steel bars and concrete in the region of shear plane. Regarding the contact between the faces of the crack, the Coulomb Friction constitutive model was considered suitable because according to international standards this criterion can determine the maximum shear stress transferred through aggregate interlock. The "shear-friction theory" can be used to predict the shear strength of different types of concrete-to-concrete interfaces and it is specific to be applied where the interfacial behavior is assumed to be controlled by cohesion (aggregate interlock), friction and dowel action. The cohesion of the Coulomb Friction interface was determined using Eq. (2) and the coefficient of friction adopted was 1.4, as suggested by Climaco and Regan (2001).

Table 3 presents the values of cohesion (c) and coefficient of friction (μ) used in the numerical model for shear plane interface and the stiffness for bond slip interface.

Table 3 Material properties of the numerical models

	Plain Concrete	Steel bars	Bond slip interface	Coulomb Frictions interface
Young's modulus (GPa)	37.96	200.0	-	-
Cohesion (c) (MPa)*	8.80	-	-	3.82
Coefficient of friction (μ)	0.84	-	-	0.80
Dilatancy Angle (degree)	0º	-	-	0º
Yielding Stress (MPa)	-	500.0	-	-
Poison (v)	0.2	0.3	-	-
Normal Stiffness Modulus (kn) (N/mm/mm³)	-	-	1000	10
Shear Stiffness Modulus (kt) (N/mm/mm³)	-	-	0.1	1000

*Cohesion (c) of concrete plain $c = f_c\left(\frac{1-\sin\phi}{2\cos\phi}\right)$

Friction angle (ϕ) of concrete plain $\phi = sin^{-1}\left(\frac{f_c-f_t}{f_c+f_t}\right)$

Cohesion (c) of Coulomb Friction interface $c = 0.25(f_c)^{2/3}$

4. Numerical results

The validation of the numerical model was done based on the shear stress versus slip behavior. The shear stress (τ) was calculated dividing the applied loading by the shear interface area (120 mm×120 mm) as performed in the experimental analysis. The maximum shear strength reached by numerical model was 6.46 MPa and the average value obtained in the push-off tests was 6.21 MPa. In the test and its numerical model, the maximum shear stress was reached when the doweling reinforcement started yielding. In Fig. 5, the shear stress versus slip curves are presented.

In general, the correlations between numerical and experimental results had satisfactorily agreement. Several parameters were involved in the calibration of the FEM model, even so the proposed combination of resources were validated and allowed the identification of significance of various effects on the response, of which the most important is the cohesion of the shear interface.

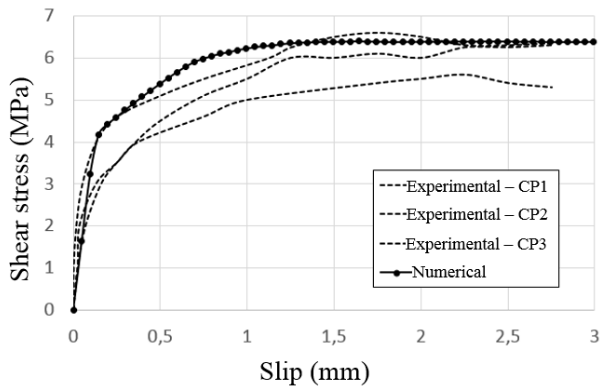

Fig. 5 Shear stress versus slip curves

Table 4 Concrete plain's properties in the parametric analysis

Properties	C30	C40	C50	C60	C70	C80	C90
Young Modulus (GPa)	31.00	35.00	40.00	42.00	43.00	45.00	47.00
Tensile Strength (MPa)	2.90	3.51	4.07	4.30	4.59	4.84	5.06
Compressive Strength (MPa)	30.00	40.00	50.00	60.00	70.00	80.00	90.00
Cohesion (c) (MPa) *	4.66	5.92	7.13	8.03	8.96	9.84	10.67
Friction angle (ϕ) (degree) *	55.48	57.00	58.15	60.03	61.29	62.37	63.31
Dilatancy Angle (degree)	0	0	0	0	0	0	0

*Cohesion (c) of concrete plain $c = f_c\left(\frac{1-\sin\phi}{2\cos\phi}\right)$

*Friction angle (ϕ) of concrete plain $\phi = sin^{-1}\left(\frac{f_c-f_t}{f_c+f_t}\right)$

The cohesion is the parameter that allows for the roughness of the interface not represented in the model. This was the reason why the width of the crack was not compared. The roughness and asperities present in the experimental test make it possible that the crack opens, which cannot be represented in the numerical model.

5. Parametric study

According to the correlation between the numerical and experimental results, it was proved that the finite element model predicted the behavior of *Z*-type push-off specimen. Therefore, to learn more about shear transfer across cracks in reinforced concrete, the effects of the cast-in-place concrete strength on the behavior of the push-off specimens were parametrically analyzed.

Concretes with 20, 25, 30, 35, 40, 50, 60, 70, 80 and 90 MPa of compressive strength were simulated. The parameters of the Coulomb Friction interface were calculated based on the concrete properties.

The tensile strength (f_{ctm}) and Young's modulus (E_{ci}) properties were calculated according to Brazilian code ABNT NBR 6118 (2014), which used Eqs. (9) and (10) for concretes with compressive strength between 20 and 50 MPa and Eqs. (11) and (12) for concretes with compressive strength between 55 and 90 MPa. Coefficient α_E is equal to 1 owing to the type of aggregate. Table 4 shows the properties used for each cast-in-place concrete.

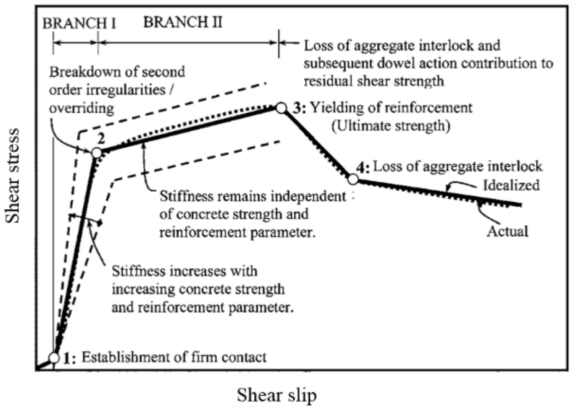

Fig. 6 Response of shear stress versus slip under increasing load by Mansur *et al*. (2008)

Table 5 Properties of the Coulomb Friction interface in the parametric analysis

Properties	C30	C40	C50	C60	C70	C80	C90
Cohesion (c) (MPa) *	2,41	2,92	3,39	3,83	4,25	4,64	5,02
Coefficient of friction (μ) *	0,8	0,8	0,8	0,8	0,8	0,8	0,8
Dilatancy Angle (degree)	0	0	0	0	0	0	0

*Cohesion (c) of Coulomb Friction interface was calculated with $c = 0.25(f_c)^{2/3}$; fc = compressive strength

$$E_{ci} = \alpha_E 5600 (f_{ck})^{1/2} \tag{9}$$

$$f_{ctm} = 0.3 (f_{ck})^{2/3} \tag{10}$$

$$E_{ci} = 21.5 \cdot 10^3 \alpha_E \left[f_{ck}/10 + 1.25 \right]^{1/3} \tag{11}$$

$$f_{ctm} = 2.12 \ln(1 + 0.11 f_{ck}) \tag{12}$$

The value of the normal and shear stiffness modulus of the Coulomb Friction interface were the same adopted in the validated model. The first one equal to 10 N/mm/mm³ and the other 1000 N/mm/mm³. The cohesion was calculated by Eq. (2) and the coefficient of friction (μ) was 1.4 as suggested by Mast (1968), Climaco and Regan (2001) and ACI Committee 318 (2008). Table 5 presents the respective values of cohesion and coefficient of friction for each concrete grade.

In reference Mansur *et al*. (2008), the load-slip response of push-off specimens was worked out with a curve presented in Fig. 6. The curve is characterized by two important branches, distinguished by a change in the slope; branch I related with concrete strength and reinforcement parameters, and branch II is related with aggregate interlock.

It the parametric results of the present numerical analyses, a similarity between the typical experimental response and the parametric simulations can be seen as shown in Fig. 7(a). An increase in concrete strength makes branch I stiffer, extending the initial linear response to a higher load level. Another important observation is the significant increase in shear strength. In branch II, the

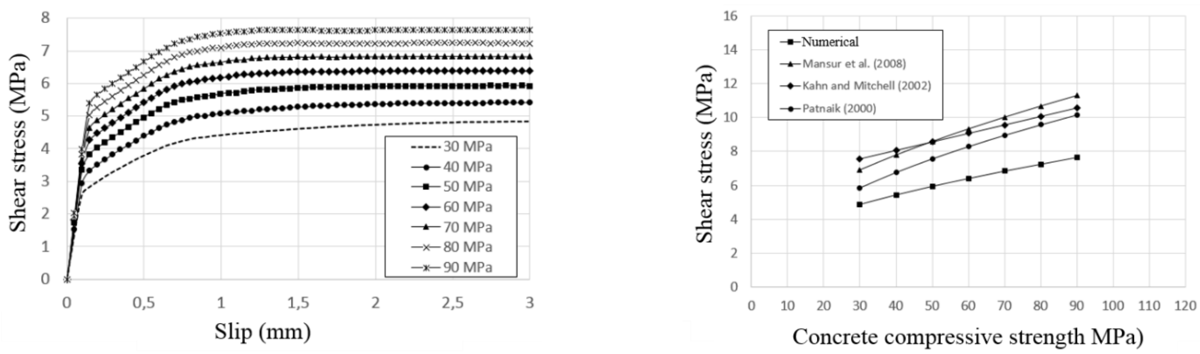

(a) Shear stress versus slip curves of the parametric study

(b) Comparison between numerical and analytical values of maximum shear stress

Fig. 7 Curves used in the parametric analysis

Table 6 Maximum shear stress values obtained by analytical predictions

Concrete compressive strength f_c (MPa)	30	40	50	60	70	80	90
Numerical (MPa)	4,86	5,43	5,94	6,39	6,83	7,24	7,64
Patnaik (2000) (MPa)	5,86	6,77	7,57	8,29	8,95	9,57	10,15
Patnaik /numerical	1,20	1,24	1,27	1,29	1,31	1,32	1,32
Kahn and Michell (2002) (MPa)	7,56	8,06	8,56	9,06	9,56	10,06	10,56
Kahn and Michell/numerical	1,55	1,48	1,44	1,41	1,40	1,38	1,38
Mansur *et al*. (2008) (MPa)	6,92	7,79	8,59	9,33	10,02	10,67	11,29
Mansur *et al*. / numerical	1,42	1,43	1,44	1,46	1,46	1,47	1,47

Patnaik (2000) $\rightarrow \tau = 0.5\sqrt{(0.25 + \rho f_y) f_c}$

Kahn & Mitchell (2002) $\rightarrow \tau = 0.05 f_c + 1.4 \rho f_y$

Mansur *et al*. (2008) $\rightarrow \tau = 0.56 f_c^{0.615} + 0.55 \rho f_y$

mechanism involved at this stage of loading is primarily governed by frictional slip. Since the coefficient of friction (μ) between concrete surfaces remains the same, the load-slip response should maintain approximately the same slope as displayed by the curves of parametric study. After branch II, it was not observed the descending branch due to as the reinforcement that crosses the shear plane is anchored in the reinforcement bars of the blocks, so that there is no pullout and no shear stress decay. The same behavior was observed by Walraven and Reinhardt (1981), Echegaray-Oviedo *et al*. (2013), Sagaseta and Vollum (2011), which state that this pattern is consistent with the constitutive law of the aggregate interlock.

According to Pul *et al*. (2017), cohesion and internal friction angles increase as the concrete strength increases and the same occurs when the maximum aggregate size is increased. However, equations for the internal friction angle as related to the concrete strength do not exist in the literature; just fixed values correlated with the interface roughness can be found.

The maximum shear stresses obtained in the numerical simulations were compared with analytical predictions proposed in by Patnaik (2000), Kahn and Mitchell (2002), Mansur *et al*. (2008). They are given as Eqs. (3), (4) and (5) and expressed in terms of concrete strength (f_c) and steel yield

Table 7 Shear stress values resulting of the proposed equation (Eq. (13))

Concrete compressive strength f_c (MPa)	Numerical (MPa)	Analytical (MPa)	Ratio
30	4,86	4,56	1,07
40	5,53	5,26	1,03
50	5,94	5,89	1,01
60	6,39	6,45	0,99
70	6,83	6,96	0,98
80	7,24	7,44	0,97
90	7,64	7,90	0,97

strength (f_y). Fig. 7(b) presents the numerical and analytical curves and Table 6 summarizes the comparison.

The maximum shear stresses obtained in the numerical simulations were compared with analytical predictions proposed in references Patnaik (2000) and Mansur *et al*. (2008). They are given as Eqs. (3), (4) and (5) and expressed in terms of concrete strength (f_c) and steel yield strength (f_y).

There is a wide variability within the values of maximum shear stresses obtained through analytical predictions. The most inadequate and unsafety analytical model is that by Kahn and Mitchell (2002). However, the analytical formulation of Patnaik (2000) provide shear stresses closer to the values obtained numerically, as can be seen in Fig. 8 and Table 6. The difference between the numerical and analytical values of shear stress is almost the same for each concrete grade. The percentage difference is varied from 20% to 32% and in the case of Mansur *et al*. (2008) the difference is about 45%.

Noting this fact, and knowing that the Patnaik (2000) formulation is aimed for monolithic concrete, a new expression suitable for cracked concrete is proposed as Eq. (13). The maximum difference between numerical and analytical result proposed in this paper was about 7% (Table 7). In addition, the experimental results were compared with the shear stress prediction calculated using the proposed equation. It was obtained that for the average of the maximum shear stress reached in the tests, the difference was 7%, and considering the specimen with the best performance, the difference was only 2%.

Based on the numerical results the Eq. (13) is proposed to determine the maximum shear stress in cracked planes of reinforced concrete with no fibers. Eq. (13) involves the

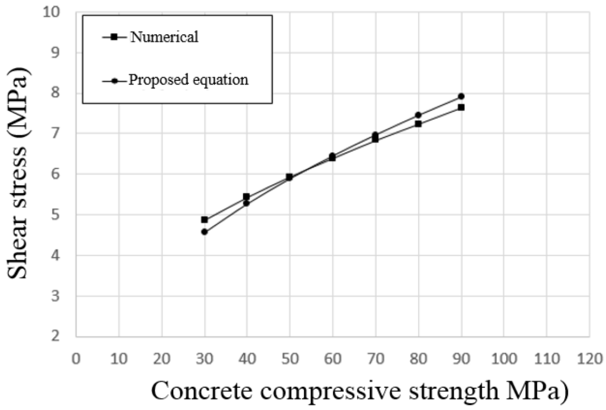

Fig. 8 Numerical and analytical curves of maximum shear stress versus concrete compressive strength proposed in this study

compressive strength of the concrete (f_c), as well as the yield strength (f_y) and the reinforcement ratio (ρ). The comparison of the numerical and analytical results proposed in this work are presented in Table 7 and Fig. 8.

$$\tau = 0{,}4\sqrt{(\rho f_y) f_c} \tag{13}$$

6. Conclusions

The shear transfer across cracks in reinforced concrete was evaluated in the present study. A three-dimensional nonlinear finite element model was constructed to represent the main features of the behavior of *Z*-type push-off specimen. The numerical analysis offers a reliable and very cost effective alternative to full-scale laboratory testing as a way of structural analysis. The concrete compressive strength was varied on parametric study in order to quantify their influence on the shear transfer across cracks. The evaluation of the results obtained in the nonlinear numerical analysis lead to the following conclusions:

• The numerical model represents satisfactorily the experimental behavior of the *Z*-type push-off specimen due to the good correlation between the shear stress versus slip curves. Based on these results, this model is considered suitable to be used as an advanced analysis tool for parametric studies;
• The adoption of the Coulomb Friction model to describe the interface in the region of shear plane provided the expected behavior. The simplified computational model with cracked surfaces discretized in terms of cohesion (c) and coefficient of friction (μ) (representing the roughness of the aggregate interlock) shows good correlation with experimental results;
• The predictions for cohesion (c) and Coefficient of friction (μ) developed in Mast (1968), Climaco and Regan (2001) and ACI Committee 318 (2008) for describing the Coulomb Friction interface provide suitable results;
• The parametric analysis, based on numerical modelling, provides important information and overcomes the disadvantages of waste time with the construction of physical models and the high cost of experimental studies.
• The proposed equation is suitable to predict the shear strength of cracked plain concrete interfaces, since the maximum difference between numerical and analytical results was only 7%.

Acknowledgments

The authors would like to thank the National Council for the Improvement of Higher Education (CAPES) and the National Council for Scientific and Technological Development (CNPq) for the financial support and the LABITECC (Laboratory of Technological Innovation in Civil Construction of the Federal University of Goiás) for running the tests.

References

ACI Committee 318 (2008), Building Code Requirements for Structural Concrete, (ACI 318M-08) and Commentary, American Concrete Institute, Farmington Hills, MI.

Arani, K.S., Zandi, Y., Pham, B.T., Mu'azu, M.A., Katebi, J., Mohammadhassani, M., Khalafi, S., Mohamad, E.T., Wakil, K. and Khorami, M. (2019), "Computational optimized finite element modelling of mechanical interaction of concrete with fiber reinforced polymer", *Comput. Concrete*, **23**(1), 61-68. https://doi.org/10.12989/cac.2019.23.1.061.

ASCE-ACI Committee 445 on Shear and Torsion (1998), "Recent approaches to shear design of structural concrete", *J. Struct. Eng.*, **124**(12), 1375-1417. https://doi.org/10.1061/(ASCE)0733-9445(1998)124:12(1375).

Associação Brasileira de Normas Técnicas. NBR 6118 (2014), Design of Concrete Structures - Procedure, Rio de Janeiro. (in Portuguese)

Bu, Z.Y., Zhang, X., Ye, H.H., Xi, K. and Wu, W.Y. (2018), "Interface shear transfer of precast concrete dry joints in segmental columns", *Eng. Struct.*, **175**, 257-272. https://doi.org/10.1016/j.engstruct.2018.08.037

Cela, J.J.L. (1998), "Analysis of reinforced concrete structures subjected to dynamic loads with a viscoplastic Drucker-Prager model", *Appl. Math. Model.*, **22**(7), 495-515. https://doi.org/10.1016/S0307-904X(98)10050-1.

Chen, W.F. (1982), *Plasticity in Reinforced Concrete*, McGraw-Hill, New York.

Climaco, J.C.T.S. and Regan, P.E. (2001), "Evaluation of bond strength between old and new concrete in structural repairs", *Mag. Concrete Res.*, **53**(6), 377-390. https://doi.org/10.1680/macr.2001.53.6.377.

Echegaray-Oviedo, J., Navarro-Gregori, J., Cuenca, E. and Serna, P. (2013), "Upgrading the push-off test to study the mechanism of shear transfer in FRC elements", *VIII International Conference on Fracture Mechanism of Concrete and Concrete structures FraMCoS-8*, Tolddo, Spain.

EN 1992-1-1 (2004), Eurocode 2 - Design of Concrete Structures - Part 1 General Rules and Rules for Buildings, European Committee for Standardization, Brussels, Belgium, 225.

Federation Internationale de la Precontrainte (FIP) (1978), Shear at the Interface of Precast and In-situ Concrete, FIP, Lausanne, Switzerland.

Hamadi, Y.D. and Regan, P.E. (1980), "Behaviour of normal and lightweight aggregate beams with shear cracks", *Struct. Eng.*,

58B(4), 71-79.

Jang, H.O., Lee, H.S., Cho, K. and Kim, J. (2018), "Numerical and experimental analysis of the shear behavior of ultrahigh-performance concrete construction joints", *Adv. Mater. Sci. Eng.*, **2018**, Article ID 6429767, 17. https://doi.org/10.1155/2018/6429767.

JSCE, JSCE-g 553e1999 (2005), Test Method for Shear Strength of Steel Fiber Reinforced Concrete, Japan Society of Civil Engineers (JSCE) Japan.

Kahn, L.F. and Mitchell, A.D. (2002), "Shear friction tests with high-strength concrete", *ACI Struct. J.*, **99**(1), 98-103.

Lee, D.H., Hwang J.H., Ju, H. and Kim, K.S. (2014), "Application of direct tension force transfer model with modified fixed-angle softened-truss model to finite element analysis of steel fiber-reinforced concrete members subjected to shear", *Comput. Concrete*, **13**(1), 49-70. https://doi.org/10.12989/cac.2014.13.1.049.

Mansur, M.A., Vinayagam, T. and Tan, K.H. (2008), "Shear transfer across a crack in reinforced high-strength concrete", *ASCE J. Mater. Civil Eng.*, **20**(4), 294-302. https://doi.org/10.1061/(ASCE)0899-1561(2008)20:4(294).

Martins, B.G. (2016), "Estudo dos mecanismos de transferência de tensões de cisalhamento em concreto fissurado com e sem reforço de fibras de aço: uma análise exploratória", Masters Dissertation, Federal University of Goiás.

Mast, R.F. (1968), "Auxiliary reinforcement in concrete connections", *ASCE J. Struct. Div.*, **94**(ST6), 1485-1504.

Mattock, A.H. (1974), "Shear transfer in concrete having reinforcement at an angle to the shear plane", *Special Publication*, **42**, 17-42.

Nielsen, M.P. (1999), *Limit Analysis and Concrete Plasticity*, 2nd Edition, CRC, CRC Press, Boca Raton, FL.

Patnaik, A.K. (2000), "Evaluation of ACI 318-95 shear-friction provisions. Discussion", *ACI Struct. J.*, **97**(3), 525-526.

Pul, S., Ghaffari, A., Öztekin, E., Hüsem, M. and Demir, S. (2017), "Experimental determination of cohesion and internal friction angle on conventional concretes", *ACI Mater. J.*, **114**(3), 407-416.

Rahal, K.N., Khaleefi, A.L. and Al-Sanee, A. (2016), "An experimental investigation of shear-transfer strength of normal and high strength self compacting concrete", *Eng. Struct.*, **109**, 16-25. https://doi.org/10.1016/j.engstruct.2015.11.015.

Sagaseta, J. and Vollum, R.L. (2011), "Influence of aggregate fracture on shear transfer through cracks in reinforced concrete", *Mag. Concrete Res.*, **63**(2), 119-137. https://doi.org/10.1680/macr.9.00191.

Santos, P.M.D. and Júlio, E.N.B.S. (2012), "A state-of-the-art review on shear-friction", *Eng. Struct.*, **45**, 435-448. https://doi.org/10.1016/j.engstruct.2012.06.036.

Soetens, T. and Matthys, S. (2017), "Shear-stress transfer across a crack in steel fibre-reinforced concrete", *Cement Concrete Compos.*, **82**, 1-13. https://doi.org/10.1016/j.cemconcomp.2017.05.010.

Spinella, N. (2013), "Shear strength of full-scale steel fibre-reinforced concrete beams without stirrups", *Comput. Concrete*, **11**(5), 365-382. http://dx.doi.org/10.12989/cac.2013.11.5.365.

Sun, C., Xiao, J. and Lange, D.A. (2018), "Simulation study on the shear transfer behavior of recycled aggregate concrete", *Struct. Concrete*, **19**, 255-268. https://doi.org/10.1002/suco.201600236.

Swamy, R.N. and Andriopoulos, A.D. (1974), "Contribution of aggregate interlock and dowel forces to the shear resistance of reinforced beams with web reinforcement", *Special Publication*, **42**, 129-168.

Taylor, H.P.J. (1970), "Investigation of the forces carried across cracks in reinforced concrete beams in shear by interlock of aggregates", British Cement Association (formerly Cement and Concrete Association), London, U.K.

TNO Building and Construction Research (2009), *Diana User's Manual*, Delft, Netherlands.

Walraven, J.C. and Reinhardt, H.W. (1981), "Concrete mechanics. Part A: Theory and experiments on the mechanical behavior of cracks in plain and reinforced concrete subjected to shear loading", *STIN*, **82**, 25417.

Wu, P., Wu, C., Liu, Z. and Hao, H. (2019), "Investigation of shear performance of UHPC by direct shear tests", *Eng. Struct.*, **183**, 780-790. https://doi.org/10.1016/j.engstruct.2019.01.055.

Xiao, J., Li, Z. and Li, J. (2014), "Shear transfer across a crack in high-strength concrete after elevated temperatures", *Constr. Build. Mater.*, **71**, 472-483. https://doi.org/10.1016/j.conbuildmat.2014.08.074.

Xiao, J., Sun, C. and Lange, D.A. (2016), "Effect of joint interface conditions on shear transfer behavior of recycled aggregate concrete", *Constr. Build. Mater.*, **105**, 343-355. https://doi.org/10.1016/j.conbuildmat.2015.12.015.

Xu, J., Wu, C., Li, Z.X. and Ng, C.T. (2015), "Numerical analysis of shear transfer across an initially uncrack reinforced concrete member", *Eng. Struct.*, **102**, 296-309. https://doi.org/10.1016/j.engstruct.2015.08.022.

CC